⌘ *Author's Choice*

THE JOURNAL OF BIOLOGICAL CHEMISTRY VOL. 287, NO. 37, pp. 31172–31184, September 7, 2012

Dynamics of Major Histocompatibility Complex Class I Association with the Human Peptide-loading Complex*[S]

Received for publication, June 1, 2012, and in revised form, July 9, 2012 Published, JBC Papers in Press, July 24, 2012, DOI 10.1074/jbc.M112.387704

Michaela S. Panter[‡§], Ankur Jain[¶], Ralf M. Leonhardt[‡], Taekjip Ha[¶‖], and Peter Cresswell[‡§1]

From the [‡]Department of Immunobiology and [§]Howard Hughes Medical Institute, Yale University School of Medicine, New Haven, Connecticut 06520-8011 and the [¶]Center for Biophysics and Computational Biology and Institute for Genomic Biology and [‖]Howard Hughes Medical Institute, University of Illinois at Urbana-Champaign, Urbana, Illinois 61801

Background: The composition of the human peptide-loading complex, required for an effective adaptive immune response, is unresolved.
Results: One peptide transporter, two tapasins, and up to two MHC I molecules are present in the complex, depending on peptide supply.
Conclusion: MHC I association with the human peptide-loading complex is dynamic.
Significance: These findings may facilitate structural and functional modeling of the complex.

Although the human peptide-loading complex (PLC) is required for optimal major histocompatibility complex class I (MHC I) antigen presentation, its composition is still incompletely understood. The ratio of the transporter associated with antigen processing (TAP) and MHC I to tapasin, which is responsible for MHC I recruitment and peptide binding optimization, is particularly critical for modeling of the PLC. Here, we characterized the stoichiometry of the human PLC using both biophysical and biochemical approaches. By means of single-molecule pulldown (SiMPull), we determined a TAP/tapasin ratio of 1:2, consistent with previous studies of insect-cell microsomes, rat-human chimeric cells, and HeLa cells expressing truncated TAP subunits. We also report that the tapasin/MHC I ratio varies, with the PLC population comprising both 2:1 and 2:2 complexes, based on mutational and co-precipitation studies. The MHC I-saturated PLC may be particularly prevalent among peptide-selective alleles, such as HLA-C4. Additionally, MHC I association with the PLC increases when its peptide supply is reduced by inhibiting the proteasome or by blocking TAP-mediated peptide transport using viral inhibitors. Taken together, our results indicate that the composition of the human PLC varies under normal conditions and dynamically adapts to alterations in peptide supply that may arise during viral infection. These findings improve our understanding of the quality control of MHC I peptide loading and may aid the structural and functional modeling of the human PLC.

The peptide-loading complex (PLC)[2] is the multimolecular functional unit of the major histocompatibility complex class I (MHC I) antigen presentation pathway. Its purpose is to load MHC I with a high affinity peptide, defined as of an optimal length for the MHC I binding groove, containing an allele-specific binding motif, and maximizing MHC I stability at the cell surface. Typically generated by the cytosolic proteasome and peptidases from intracellular pathogens or endogenous proteins in nucleated cells, peptides of 8–20 amino acids are readily translocated into the endoplasmic reticulum (ER) lumen by the transporter associated with antigen processing (TAP). Following trimming by ER-associated aminopeptidases 1 and 2 to a length of 8–10 amino acids, peptide binding to MHC I triggers its dissociation from the PLC and export to the cell surface for presentation to cytotoxic T lymphocytes. In contrast, suboptimal MHC I assembly, for example upon viral inhibition of TAP, leads to its ER retention (1–3) and proteasomal degradation (4).

The numerous interactions between the PLC components all contribute to a unique peptide optimization mechanism. The ATP-dependent TAP heterodimer, comprising the TAP1 and TAP2 subunits, interacts with the chaperone tapasin via its N-terminal domains (5, 6), enhancing TAP stabilization, expression, and peptide translocation (7–9). By binding TAP, tapasin also serves as a bridge between MHC I and the transporter, facilitating peptide loading (10). Tapasin additionally stabilizes empty MHC I molecules (11), promotes their ER retention (12), and catalyzes as well as optimizes MHC I loading with peptides (13–17). The latter editing function may be accomplished by disrupting noncovalent interactions between the MHC I binding groove and a suboptimal peptide, returning MHC I to a peptide-receptive conformation (16). These stabilizing and editing functions require that tapasin is covalently linked, via a disulfide bond, to the protein-disulfide isomerase

* This work was supported, in whole or in part, by National Institutes of Health Grants AI083025 and GM065367 (to T. H.) and Training Grant T32AI07019 (to the Yale Department of Immunobiology). This work was also supported by the Howard Hughes Medical Institute and a Cancer Research Institute Fellowship (to R. M. L.).
⌘ *Author's Choice*—Final version full access.
[S] This article contains supplemental Fig. S1.
[1] To whom correspondence should be addressed: Dept. of Immunobiology, Yale University School of Medicine, 300 Cedar St., TAC S670, New Haven, CT 06520-8011. Tel.: 203-785-5176; Fax: 203-737-1764; E-mail: peter.cresswell@yale.edu.

[2] The abbreviations used are: PLC, peptide-loading complex; MHC I, major histocompatibility complex class I; ER, endoplasmic reticulum; TAP, transporter associated with antigen processing; CRT, calreticulin; CFP, cyan fluorescent protein; GILT, γ-interferon-inducible lysosomal thiol reductase; CHX, cycloheximide; MMTS, methyl methanethiosulfonate; SiMPull, single-molecule pulldown; β_2m, β_2-microglobulin; HC, heavy chain.

ERp57 (15). This tapasin-ERp57 heterodimer increases MHC I and calreticulin (CRT) recruitment into the PLC by linking the MHC I-binding site on tapasin and the CRT-binding site on ERp57 (15).

Although the functions of the PLC constituents are increasingly well understood, their stoichiometry is still controversial. Although the MHC I/CRT, tapasin/ERp57, and TAP1/TAP2 ratios have all been confirmed to be 1:1 (18–22), past reports have variously defined the TAP/tapasin/MHC I ratio as 1:1:1 (23), 1:4:4 (3, 24), and a mixture of 1:2:0 and 1:2:1 (21). The 1:2:1 ratio has been bolstered by studies of chimeric human cells expressing rat TAP (6, 21, 25) but has not been corroborated in a normal human cell line. In this study, we examined the stoichiometry of the human PLC, focusing on the TAP/tapasin and tapasin/MHC I ratios. Using a single-molecule approach, we confirm that the TAP/tapasin ratio is 1:2 in a human cell line, as suggested previously by studies using insect-cell microsomes (5), rat-human chimeric cells (6, 21, 25), and truncated TAP-expressing HeLa cells (26). We also demonstrate that the composition of the MHC I-associated human PLC varies, including subpopulations with a tapasin/MHC I ratio of 2:1 or 2:2. In addition, the PLC stoichiometry appears to be dynamic, with increased MHC I binding to tapasin when the peptide supply is decreased by inhibition of the proteasome or TAP. These findings advance our understanding of the molecular composition of the PLC, providing insight into the quality control of MHC I antigen presentation both under normal conditions and during the adaptive immune response, as well as potentially facilitating modeling of the not-yet-crystallized PLC.

EXPERIMENTAL PROCEDURES

Cell Lines—The human B-cell lines .220.B4402 (27), 45.1 (28), .174 (28), 45.1.ICP47 (4), Daudi (29), Daudi.β_2m (30), T2 (31), and C1R (32), as well as any derivatives and 293T (33), were cultured in Iscove's modified Dulbecco's medium (Sigma) supplemented with 10% bovine calf serum (HyClone), 2% Glutamax (Invitrogen), and 1% penicillin/streptomycin (Invitrogen). HeLaM cells (34) and their derivatives were grown in Dulbecco's modified Eagle's medium (Sigma) supplemented as above and stimulated with 200 units/ml recombinant human IFN-γ (PeproTech) for 48 h before each experiment. T2 cells transfected with wild-type (1WT) or Walker A-motif lys to ala mutant (1K>A) human TAP1 and wild-type (2WT) or Walker A-motif mutant lys to ala (2K>A) human TAP2 were cultured in selection medium, as described previously (35). T2 cells transfected with rat TAP1 and TAP2 (a kind gift from Dr. Michael Knittler, Friedrich-Loeffler-Institut, Tuebingen, Germany) were also maintained as reported previously (36).

Antibodies—All antibodies were previously generated by us or in other laboratories, with the exception of the commercially available antibodies rat anti-human GRp94 (9G10; Enzo Life Sciences), mouse anti-GFP (3E6; Invitrogen), mouse anti-GFP (JL-8; Clontech), mouse anti-His (ab18184; Abcam), rabbit anti-His (ab9108; Abcam), mouse anti-human TAP2 (K0137-3; MBL International), biotinylated goat anti-GFP (600-106-215; Rockland Immunochemicals), and biotinylated mouse anti-FLAG (F9291; Sigma). Based on the product information, the anti-GFP antibodies 3E6 and JL-8 are reactive with cyan fluorescent protein (CFP), and the biotinylated goat anti-GFP antibody has been shown to react with yellow fluorescent protein (YFP) (37, 38). All secondary antibodies used for flow cytometry (goat anti-mouse IgG coupled to AlexaFluor488, AlexaFluor647, or FITC and goat anti-rabbit IgG coupled to AlexaFluor647) were purchased from Invitrogen, and those for immunoblotting (goat anti-mouse and anti-rat IgG coupled to horseradish peroxidase and goat anti-mouse, anti-rat, and anti-rabbit IgG coupled to alkaline phosphatase) were purchased from Jackson ImmunoResearch. The anti-human TAP1 antibodies 148.3 (22) and R.RING4C (22); the anti-human tapasin antibodies PaSta1 (39), PaSta2 (40), R.Gp48C (7), and R.SinA (41); the anti-human MHC I antibodies 3B10.7 (42), 4E (43), BB7.2 (44), HC10 (45), and W6/32 (46); and the anti-human γ-interferon-inducible lysosomal thiol reductase (GILT) antibody MaP.IP30 (47), used as an immunoprecipitation control, have been reported previously. The rabbit antibody D90 was raised against the C-terminal epitope of rat TAP1 (CYRSMVEALAAPSD) as described previously (48) (Thermo Scientific Open Biosystems).

Retroviral Constructs—The introduction of tapasin-YFP into the pLPCX retroviral vector (Clontech), with YFP at the C terminus of tapasin, has been described previously (49). HLA-A0201-CFP was also tagged at the C terminus and expressed in the pLPCX vector (a kind gift from Dr. David Stepensky, Ben-Gurion University, Beersheba, Israel). HLA-A0201 in the pBMN-IRES-neo retroviral vector (a kind gift from Dr. Nathalie Vigneron, Ludwig Institute for Cancer Research, Brussels, Belgium) served as a template for QuikChange site-directed mutagenesis (Stratagene) using the primer pair 5′-GCTTGTAAAGTGCACCATCACCATCACCATTGAG-AATTCCAG-3′ and 5′-GCTGGAATTCTCAATGGTGATG-GTGATGGTGCACTTTACAAGC-3′, with the goal of introducing a C-terminal His tag onto HLA-A0201. US6-FLAG in the pCDNA3 vector (a kind gift from Dr. Paul Lehner, University of Cambridge, Cambridge, UK) (50) was also subjected to mutagenesis using the primer pair 5′-TTGAATTCATGGAC-CTCTTGATCCGTCTCGG-3′ and 5′-AAGAATTCTCAGG-AGCCACAACGTCGAATC-3′. Following purification with a QIAquick® PCR purification kit (Qiagen), digestion with EcoRI (New England Biolabs), and repurification, US6 was ligated into pBMN-IRES-neo. To generate N-terminally truncated TAP1 (1ΔN), human TAP1 in the pLPCX vector served as a template for mutagenesis using the primer pair 5′-GCTTCGGGATCC-TGCCGCCACCATGCCCGGGGGTCAGGGCGGCTCTGG-3′ and 5′-CCAGAGCCCTGACCCCCGGGCATGGTGGCG-GCAGGATCCCGAAGC-3′, and human TAP2 in the pLNCX2 retroviral vector (Clontech) served as a template for mutagenesis using the primer pair 5′-CGCGGCTGAGCCGCCACCA-TGCCCGGGGCCCAGGAGAAGG-3′ and 5′-CCTTCT-CCTGGGCCCCGGGCATGGTGGCGGCTCAGCCGCG-3′ to generate N-terminally truncated TAP2 (2ΔN). Following purification, digestion with XhoI and NotI (New England Biolabs), and repurification, full-length TAP1 and 1ΔN were ligated into the pBMN-IRES-EGFP retroviral vector (20), respectively. Sequencing of each construct was performed prior to retroviral transduction.

Retroviral Transduction—In all cases, retrovirus was generated in 293T cells transfected with 4 μg/ml of the packaging vector pCL-Ampho (Imgenex) and the construct of interest and 20 μg/ml Lipofectamine 2000 (Invitrogen) in Opti-MEM (Invitrogen), followed by three rounds of retroviral transduction of a recipient suspension cell line with 8 μg/ml polybrene (Millipore) or of a recipient adherent cell line with 3 μg/ml Lipofectamine 2000. Stably expressing cells were obtained by selection in complete medium supplemented with 500 ng/ml (.220.B4402.tapasin-YFP) or 750 ng/ml (HeLaM.A2-CFP) puromycin (Sigma) or 2 mg/ml G418 (Invitrogen) (C1R.A2-His and 45.1.US6). The 45.1.US6 cell line was additionally sorted for low surface HLA-B and -C expression using a FACSAria (BD Biosciences). T2 cells expressing full-length TAP1 or 1ΔN were sorted for high GFP expression, cloned by limiting dilution, and then transduced with full-length TAP2 or 2ΔN. The resultant T2 variants were selected in complete medium supplemented with 2 mg/ml G418 and cloned by limiting dilution. In all cases, cellular phenotypes were confirmed by flow cytometry and/or immunoblotting.

Flow Cytometry—For surface flow cytometry, cells were sequentially labeled with primary and secondary antibody in 1% bovine calf serum in 1× PBS on ice, unless the protein of interest was fluorescently tagged with YFP and analyzed using a FACSCalibur (BD Biosciences) and FlowJo software (Tree Star). For intracellular flow cytometry, cells were fixed in 3% formaldehyde with 10 mM HEPES in 1× PBS. In some cases, fixation was preceded by treatment with the cell-permeable proteasome inhibitor lactacystin (EMD4Biosciences) at 20 μM or 10 μg/ml of the protein synthesis inhibitor cycloheximide (CHX; Sigma) for 2.5 h in complete medium. Following two washes, the cells were sequentially labeled with primary and secondary antibody in 1% bovine calf serum and 0.5% saponin in 1× PBS. The ratio of the mean PaSta2 or anti-TAP1 fluorescence to the mean PaSta1 fluorescence was then quantitated using FlowJo software.

Immunoprecipitation and Immunoblotting—Cells were pretreated with 10 mM methyl methanethiosulfonate (MMTS; Thermo Scientific) and lysed in 1% digitonin (EMD4Biosciences) in 1× TBS (150 mM sodium chloride, 25 mM Tris, pH 7.4) supplemented with 2 mM MMTS, 1 mM calcium chloride, and Complete Mini, EDTA-Free Protease Inhibitor Cocktail (Roche Applied Science) for 15–30 min on ice. Post-nuclear lysates were then either prepared for SDS-PAGE by the addition of reducing (100 mM dithiothreitol; American Bioanalytical) sample buffer or precleared with protein G-Sepharose (GE Healthcare) or protein A-Sepharose (Sigma) for 1 h, followed by immunoprecipitation using the same beads and the indicated antibody. In the case of depleting immunoprecipitation, the lysate was sequentially immunoprecipitated four times with PaSta1 or PaSta2, followed by a fifth immunoprecipitation with either the same antibody or its counterpart. To prevent antibody carryover, the antibody was pre-bound to the beads for 1 h, and any excess antibody was removed by washing with 1× TBS. After three washes in 0.1% digitonin lysis buffer and elution in nonreducing sample buffer, the immunoprecipitates were separated by SDS-PAGE. Standard or quantitative immunoblotting was then performed as described previously (15, 19, 51).

Metabolic Labeling and Immunoprecipitation—Cells were incubated in cysteine- and methionine-free Dulbecco's modified Eagle's medium supplemented with 3% dialyzed fetal bovine serum (Invitrogen), 1% Glutamax, 1% penicillin/streptomycin, and 2% HEPES (Invitrogen) for 1 h, followed by labeling with [^{35}S]methionine/cysteine (PerkinElmer Life Sciences) in the same medium for 2 h. The cells were then pretreated with 10 mM MMTS, lysed, and immunoprecipitated as described above, with the addition of normal rabbit serum (Invitrogen) to the preclear step. After separation by SDS-PAGE, each gel was fixed, dried, and exposed to a PhosphorImager screen (GE Healthcare) before scanning using a Storm 860 PhosphorImager (GE Healthcare) and analysis using ImageQuant software (GE Healthcare).

Single-molecule Pulldown (SiMPull)—SiMPull was performed as described previously (37, 38). Briefly, .220.B4402.tapasin-YFP cells were lysed as detailed above and diluted as necessary in 1% digitonin lysis buffer. The cell lysates were then applied to slides coated with biotinylated antibody, and immobilized complexes were assessed for YFP fluorescence using a total internal reflection fluorescence microscope with single-fluorophore sensitivity and custom software. Following pulldown with the anti-TAP1 antibody 148.3, if each PLC contains a single tapasin-YFP molecule, all visualized complexes would be expected to exhibit one-step photobleaching. As ~75% of YFP is fluorescently active (37, 52), if each PLC composes two YFP-tagged tapasin molecules, 38% of all complexes would be expected to photobleach in one step and 56% in two steps, as a result of one or both fluorophores being active, respectively. Accounting for 6% of complexes that would contain two inactive fluorophores and thus would not be observable, these cited values correspond to 40 and 60% of observed complexes, respectively. In this way, the SiMPull technique allows accurate quantitation of the TAP/tapasin ratio.

Affinity Purification and Size-exclusion Chromatography—Affinity purification of the PLC was performed by applying HeLaM.A2-CFP digitonin lysate to mouse IgG-agarose (Sigma) and cyanogen bromide-activated, 148.3-coupled Sepharose 4B (GE Healthcare) columns in series. The bound complexes were competitively eluted with 100 μM RING4C peptide (CYWAMVQAPADAPE; Immuno Dynamics), the C-terminal TAP1 epitope against which the antibody 148.3 was raised (24, 53), in 1% digitonin lysis buffer. Immunoprecipitation of the affinity-purified PLCs or size-exclusion chromatography was then performed. Briefly, a Superdex 200 10/60 column (120-ml elution volume and 39.8-ml void volume; GE Healthcare) was equilibrated and calibrated using proteins with known Stokes radii in 0.1% digitonin lysis buffer at 4 °C and a flow rate of 1 ml/min, followed by injection of 1 ml of the affinity-purified material. The resultant fractions were analyzed by SDS-PAGE and quantitative immunoblotting. The Stokes radius of the PLC was then calculated from the calibration and quantitative immunoblotting data according to the manufacturer's instructions.

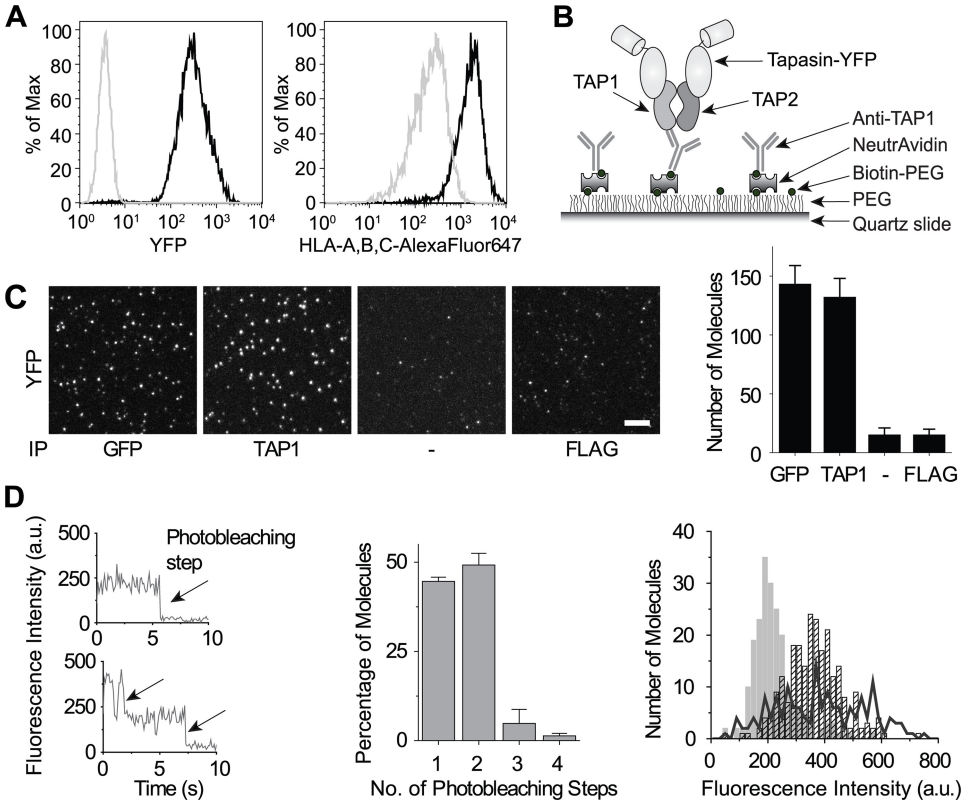

FIGURE 1. **TAP/tapasin ratio is 1:2 in human cells.** *A*, tapasin-negative (*gray line*) or tapasin-YFP-expressing (*black line*) .220.B4402 cells directly analyzed by flow cytometry for YFP fluorescence (*left panel*) or labeled with W6/32 (anti-HLA-A, -B, and -C) and AlexaFluor647-coupled goat anti-mouse IgG to assess MHC I surface expression (*right panel*). *B*, schematic depicting SiMPull analysis of .220.B4402.tapasin-YFP cells. Cells were lysed in digitonin and applied to an antibody-coated slide, followed by imaging using a total internal reflection fluorescence microscope. *C*, representative fluorescent images (*left panel*) and quantitation (*right panel*) of tapasin-YFP pulldown in slides coated with goat anti-GFP, the anti-TAP1 antibody 148.3, no antibody, or a control antibody (mouse anti-FLAG). To achieve an optimal density of molecules for imaging, the .220.B4402.tapasin-YFP lysate was diluted 1000-fold (anti-GFP), 20-fold (anti-TAP1), or 10-fold (no antibody and anti-FLAG) in 1% digitonin lysis buffer. The *scale bar* on the fluorescent images represents 5 μm. The quantitative results are expressed as the means plus the S.D. of at least 20 imaging areas (2500 μm^2 each) in one representative experiment. *D*, representative fluorescence time traces of molecules exhibiting one-step (*top left panel*) and two-step (*bottom left panel*) photobleaching, photobleaching step distribution (*middle panel*), and fluorescence intensity distribution (*right panel*) for the observed tapasin-YFP photobleaching events following pulldown with the anti-TAP1 antibody 148.3. The photobleaching step distribution data are expressed as the means plus the S.D. of three independent experiments, with at least 500 molecules scored per experiment. *Solid bars*, molecules exhibiting one-step photobleaching. *Hatched bars*, molecules exhibiting two-step photobleaching. *Line*, rejected molecules. *PEG*, polyethylene glycol. *IP*, immunoprecipitation. *a.u.*, arbitrary units.

RESULTS

The TAP/Tapasin Ratio Is 1:2 in Human Cells—To determine the TAP/tapasin ratio in human cells expressing human TAP, we transduced YFP-tagged tapasin into the tapasin-negative .220.B4402 cell line (Fig. 1*A*, *left panel*), which restored MHC I surface expression (Fig. 1*A*, *right panel*), for single-molecule analysis using the SiMPull technique (37, 38). Briefly, digitonin lysates of these cells were applied to slides coated with biotinylated antibody to capture PLCs, and YFP photobleaching was examined by total internal reflection fluorescence microscopy, as described previously (Fig. 1*B*) (37, 38). Specific pulldown of tapasin-YFP using anti-GFP or the anti-TAP1 antibody 148.3 was demonstrated in comparison with slides coated with a control or no antibody (Fig. 1*C*). The nearly equal numbers of one- and two-step photobleaching events (Fig. 1*D*, *left* and *middle panels*) following 148.3 pulldown matched the binomial distribution predicted for a 1:2 TAP/tapasin-YFP ratio (37), given that only ~75% of YFP is fluorescently active (see "Experimental Procedures") (37, 52). Additionally, the initial fluorescence intensity of the molecules exhibiting two-step photobleaching was twice that of the molecules photobleaching in a single step (Fig. 1*D*, *right panel*), indicating accurate scoring of the fluorescence time traces, while the broad distribution of the 25% of traces that were not interpretable (Fig. 1*D*, *right panel*) is consistent with a lack of scoring bias. In the past, the TAP/tapasin ratio has been suggested to be 1:2 (21, 26), particularly due to the presence of one tapasin-binding site on each subunit of rat TAP (6, 21). Our SiMPull data confirm that the TAP/tapasin stoichiometry is 1:2 in human cells expressing human TAP.

A PLC Subpopulation Is Differentially Reactive with Two Anti-tapasin Antibodies—SiMPull could not be employed to determine the tapasin/MHC I ratio because there are no completely MHC I-negative human cell lines available for transduction with YFP-tagged MHC I. As an alternative, the antibodies PaSta1 and PaSta2 were used to characterize MHC I association with tapasin. PaSta1 is reactive with all tapasin (39), while PaSta2 is unable to bind MHC I-associated tapasin because its epitope is located at the MHC I-tapasin interface (40). To verify this binding difference using cell lysates rather than purified protein (40), we compared PaSta1- and PaSta2-immunoprecipitated PLCs from the normal B-cell line 45.1 and its TAP-negative derivative .174, which accumulates subcomplexes

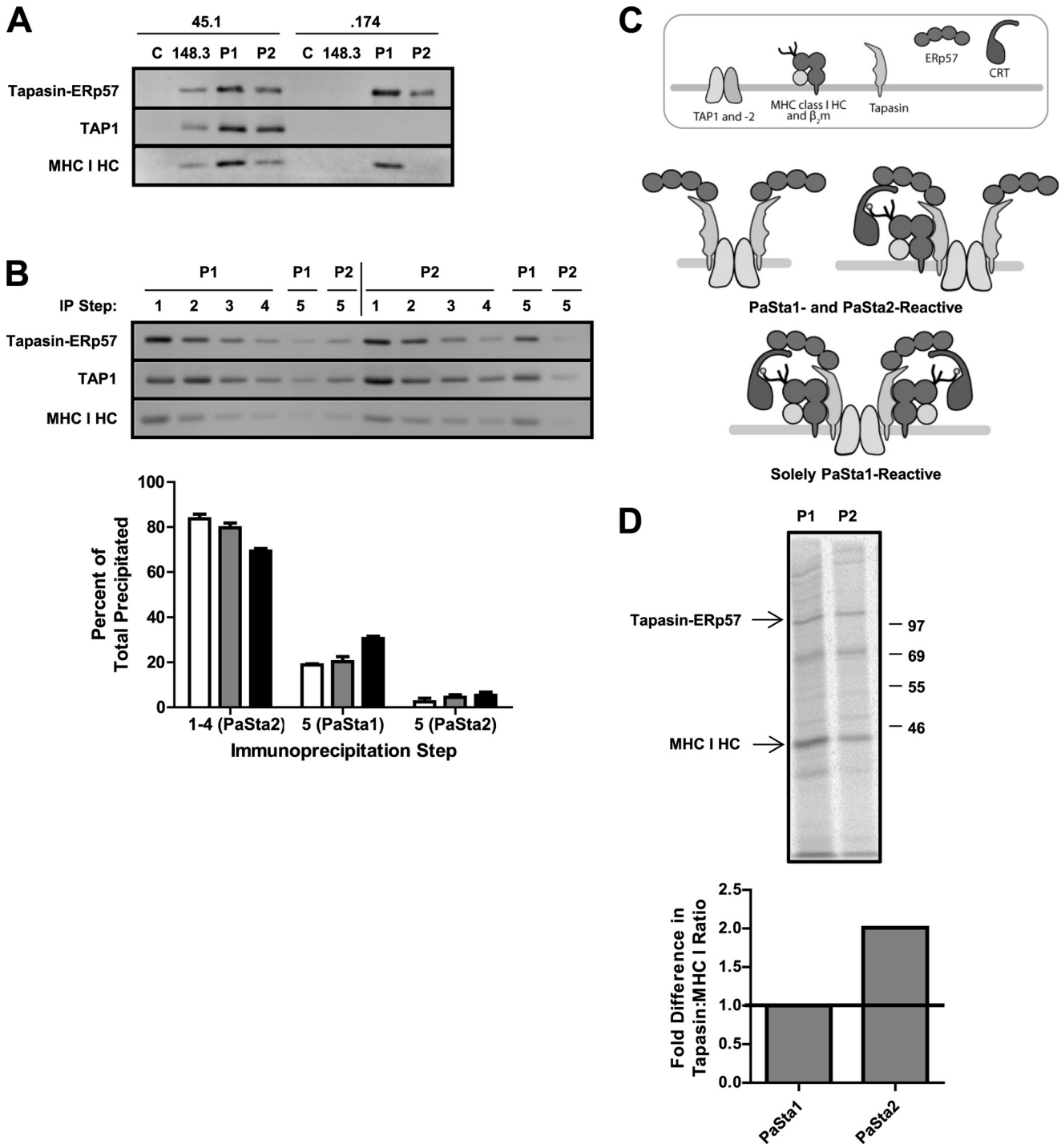

FIGURE 2. **PLC subpopulation is differentially reactive with the anti-tapasin antibodies PaSta1 and PaSta2.** *A*, digitonin lysates of wild-type 45.1 and TAP-negative .174 cells were immunoprecipitated with the indicated antibodies, separated by SDS-PAGE, and immunoblotted with R.SinA (anti-tapasin), R.RING4C (anti-TAP1), and 3B10.7 (anti-MHC I heavy chain (*HC*)). MaP.IP30 (anti-GILT) served as a negative control for the immunoprecipitation. *B*, 45.1 digitonin lysate was sequentially immunoprecipitated with either PaSta1 or PaSta2, followed by a fifth immunoprecipitation with either of the antibodies. After SDS-PAGE and immunoblotting with R.Gp48C (anti-tapasin), R.RING4C (anti-TAP1), and 3B10.7 (anti-MHC I HC), the bands were quantitated. These results are expressed as the means plus the S.D. of three independent experiments. *White bars*, tapasin-ERp57. *Gray bars*, TAP1. *Black bars*, MHC I HC. *C*, schematic of both PaSta1- and PaSta2-reactive PLCs and a solely PaSta1-reactive PLC. *D*, radiolabeled 45.1 digitonin lysate was immunoprecipitated with the indicated antibodies (*top panel*), and the resultant tapasin-ERp57 and MHC I HC bands were quantitated (*bottom panel*). The relative tapasin/MHC I ratios of the PLC subpopulations precipitated by PaSta1 and PaSta2, respectively, were then calculated and normalized to that of PaSta1. These results are expressed as the means plus the S.D. of five independent experiments. *C*, control antibody. *P1*, PaSta1. *P2*, PaSta2. *HC*, heavy chain. *IP*, immunoprecipitation.

containing tapasin-ERp57, CRT, and MHC I (54). As expected, in the absence of TAP, PaSta2 was unable to precipitate MHC I-bound tapasin (Fig. 2*A*), confirming that PaSta2 and MHC I binding to tapasin is mutually exclusive.

To compare the PLC subpopulations bound by PaSta1 and PaSta2, 45.1 digitonin lysate was subjected to four sequential immunoprecipitations with one antibody, followed by a fifth immunoprecipitation with the same antibody or its counter-

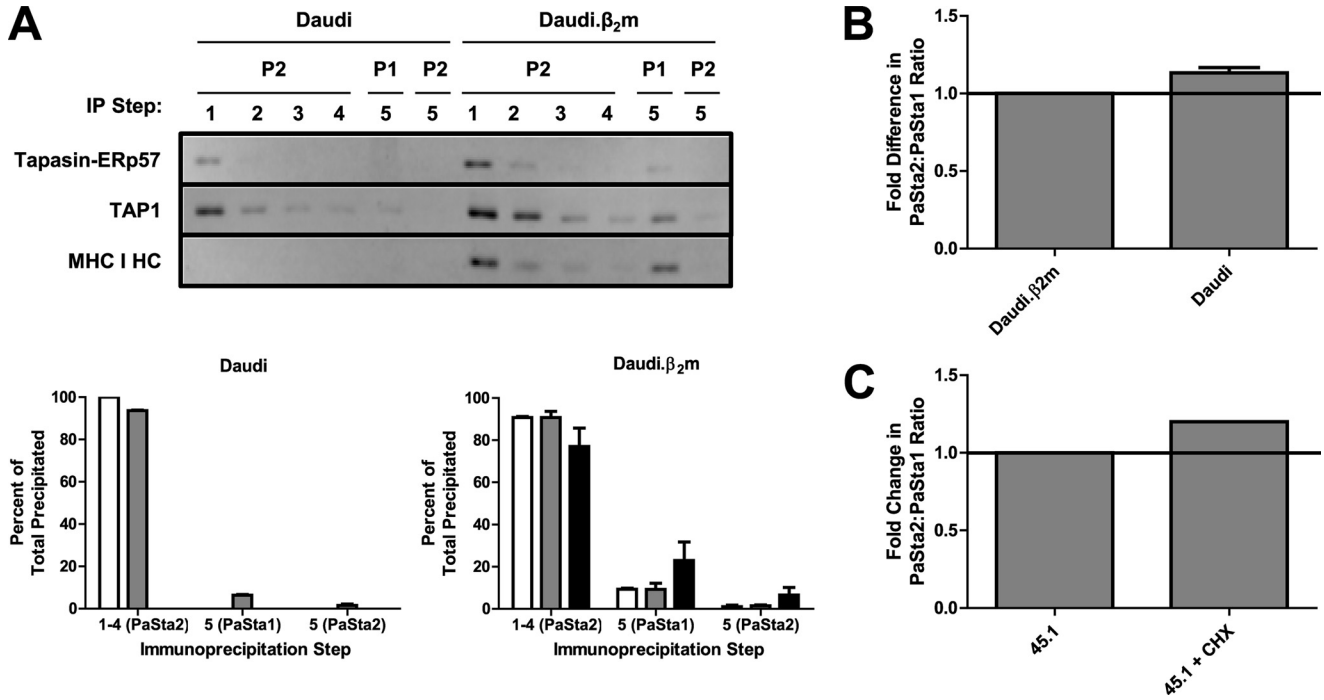

FIGURE 3. **Discrepancy in PaSta1 and PaSta2 binding is MHC I-dependent and detergent-independent.** *A*, Daudi (*left*) and Daudi.β_2m (*right*) digitonin lysates sequentially immunoprecipitated with PaSta2, followed by a fifth immunoprecipitation with PaSta1 or PaSta2. After SDS-PAGE and immunoblotting with R.Gp48C (anti-tapasin), R.RING4C (anti-TAP1), and 3B10.7 (anti-MHC I HC) (*top*), the bands were quantitated (*bottom*). These results are expressed as the means plus the S.D. of two independent experiments. *White bars*, tapasin-ERp57. *Gray bars*, TAP1. *Black bars*, MHC I HC. Daudi and Daudi.β_2m cells (*B*) or untreated and CHX-treated (10 μg/ml for 2.5 h) 45.1 cells (*C*) were fixed in formaldehyde, permeabilized in saponin, and labeled with PaSta1 or PaSta2 and AlexaFluor488-coupled goat anti-mouse IgG prior to intracellular flow cytometry analysis. A negative control, labeled only with secondary antibody, was also included. The ratio of PaSta2/PaSta1 binding following background subtraction was then calculated. These results are expressed as the means plus the S.D. of three (*B*) or two (*C*) independent experiments. In representative experiments, the ratio of the mean PaSta2 fluorescence to the mean PaSta1 fluorescence before normalization was 1.01 for Daudi.β_2m cells and 1.23 for Daudi cells (*B*) and 0.87 for untreated 45.1 cells and 1.01 for CHX-treated 45.1 cells (*C*). *P1*, PaSta1. *P2*, PaSta2. *IP*, immunoprecipitation. *HC*, heavy chain.

part. When the PLC population was depleted of PaSta2-reactive complexes, a subpopulation remained that was solely recognized by PaSta1 (Fig. 2*B*). However, the reciprocal experiment did not yield a significant residual PLC subpopulation reactive with either antibody (Fig. 2*B*, *top panel*). Approximately 20% of all precipitated tapasin-ERp57 and TAP1 and 30% of all precipitated MHC I were included in the solely PaSta1-reactive subpopulation (Fig. 2*B*, *bottom panel*), consistent with both tapasin molecules in these complexes being occupied by MHC I. This effect was not diminished by TAP2 or tapasin overexpression (data not shown), excluding the possibility of incompletely assembled PLCs. The differential reactivities of PaSta1 and PaSta2 with the PLC population were also observed in several other human cell lines, including Daudi.β_2m (Fig. 3*A*), T2-expressing human TAP1 and TAP2 (Fig. 4*B*), and C1R (Fig. 6*B*). Based on the inability of PaSta2 to recognize a subset of complexes, as well as the higher percentage of total precipitated MHC I than tapasin-ERp57 and TAP1 in that subset (Fig. 2*B*, *bottom panel*), we hypothesized that the PLC population is heterogeneous, containing zero, one, or two MHC I molecules per complex (Fig. 2*C*).

The relative tapasin/MHC I ratios of the PLC subpopulations precipitated by PaSta1 and PaSta2 were verified by immunoprecipitating radiolabeled 45.1 digitonin lysate with the two antibodies, followed by tapasin-ERp57 and MHC I band quantitation. The tapasin/MHC I ratio of the subpopulation precipitated by PaSta2 was 2-fold higher than that of the complexes detected by PaSta1 in five independent experiments (Fig. 2*D*), consistent with the existence of MHC I-saturated complexes unable to bind PaSta2 (Fig. 2*C*).

To confirm that the difference in PaSta1 and PaSta2 binding was MHC I-dependent, depleting immunoprecipitations were performed on digitonin-lysed Daudi cells, which lack β_2-microglobulin (β_2m) expression and thus MHC I association with the PLC, and their reconstituted counterpart Daudi.β_2m. Whereas PaSta1 precipitated a PLC subpopulation from Daudi.β_2m cells that was not reactive with PaSta2, comprising ~10% of all precipitated tapasin-ERp57 and TAP1 (Fig. 3*A*, *right*), the two antibodies exhibited similar reactivities in Daudi cells (Fig. 3*A*, *left*). This result was consistent with a 13% higher PaSta2/PaSta1 binding ratio in Daudi cells than in Daudi.β_2m cells examined by intracellular flow cytometry (Fig. 3*B*), suggesting that the difference in antibody binding in these two cell types is due to MHC I obstruction of the PaSta2 epitope and not an artifact of detergent-induced PLC aggregation or PaSta2 epitope degradation. Moreover, free, non-PLC-associated tapasin does not account for the difference in PaSta1 and PaSta2 reactivity, as the anti-TAP1/PaSta1 binding ratio was approximately equal between Daudi and Daudi.β_2m cells (data not shown). The MHC I dependence of the discrepancy in PaSta1 and PaSta2 binding to the PLC was further supported by an increased PaSta2/PaSta1 binding ratio in 45.1 cells treated with CHX to block protein and hence MHC I synthesis (Fig. 3*C*). This treat-

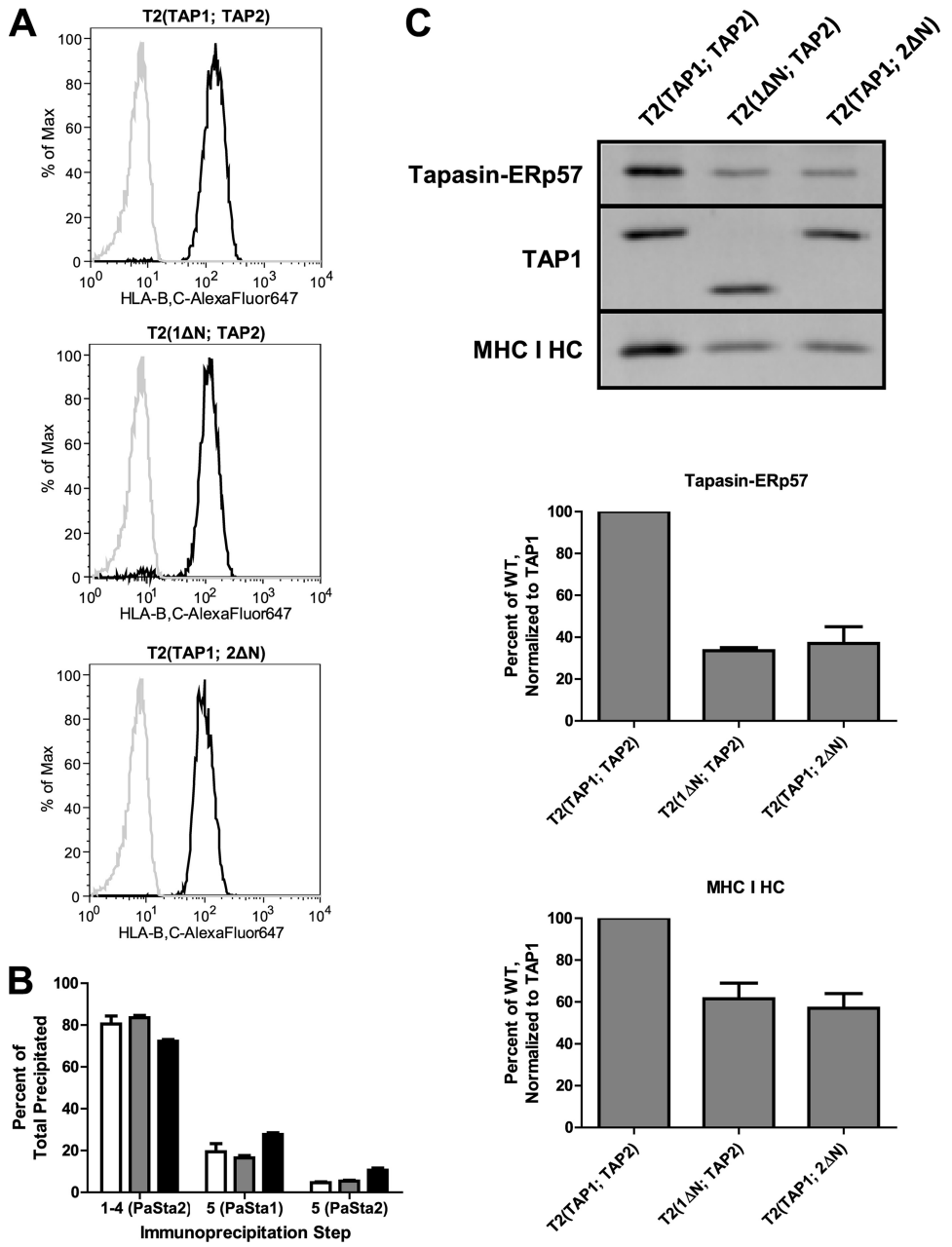

FIGURE 4. **Mutant TAP analysis indicates that two MHC I molecules can associate with a single human PLC.** *A*, TAP-negative T2 cells (*gray line*) and T2 cells expressing full-length TAP1 and full-length TAP2 (T2(TAP1; TAP2)), 1ΔN and full-length TAP2 (T2(1ΔN; TAP2)), or full-length TAP1 and 2ΔN (T2(TAP1; 2ΔN)), (*black line*) were labeled with 4E (anti-HLA-B and -C) and AlexaFluor647-coupled goat anti-mouse IgG and analyzed by flow cytometry for MHC I surface expression. *B*, T2(TAP1; TAP2) digitonin lysate sequentially immunoprecipitated with PaSta2, followed by a fifth immunoprecipitation with PaSta1 or PaSta2. After SDS-PAGE and immunoblotting with R.Gp48C (anti-tapasin), R.RING4C (anti-TAP1), and 3B10.7 (anti-MHC I HC), the bands were quantitated. These results are expressed as the means plus the S.D. of two independent experiments. *White bars*, tapasin-ERp57. *Gray bars*, TAP1. *Black bars*, MHC I HC. *C*, T2(TAP1; TAP2), T2(1ΔN; TAP2), and T2(TAP1; 2ΔN) digitonin lysates immunoprecipitated with anti-TAP2, separated by SDS-PAGE, and immunoblotted with R.SinA (anti-tapasin), R.RING4C (anti-TAP1), and 3B10.7 (anti-MHC I HC) (*top*). The bands were then quantitated, and tapasin-ERp57 (*middle*) and MHC I HC (*bottom*) levels were normalized to TAP1 expression and expressed as a percentage of T2(TAP1; TAP2). These results are expressed as the means plus the S.D. of two independent experiments. *HC*, heavy chain.

ment likely resulted in lower MHC I association with the PLC, leading to increased PaSta2 binding (Fig. 2*C*).

Two MHC I Molecules Can Associate with a Single Human PLC—The differential recognition of PLC subpopulations by PaSta1 and PaSta2 does not exclude the possibility of PaSta2 epitope obstruction by a conformational change in tapasin or by the association of a protein other than MHC I. To address this issue, two independent approaches were implemented. In the first approach, N-terminally truncated human TAP1 (1ΔN) and TAP2 (2ΔN) were co-expressed with full-length human TAP2 or TAP1, respectively, in T2 cells. These mutant transporters were functional, as indicated by MHC I surface expression equal to that of T2 cells expressing full-length TAP1 and TAP2 (Fig. 4*A*). As expected, T2 cells expressing full-length TAP exhibited a discrepancy in PaSta1- and PaSta2-reactive PLCs using the same depleting immunoprecipitation technique

that we employed to examine 45.1 cells (Fig. 4*B*). However, anti-TAP2 immunoprecipitation, performed to ensure that fully assembled complexes were being sampled rather than single-chain TAP1 (55), revealed that tapasin association with the PLC was reduced in T2 cells expressing 1ΔN or 2ΔN (Fig. 4*C*, *top* and *middle panels*). Similarly, MHC I binding to the PLC was decreased (Fig. 4*C*, *top* and *bottom panels*), consistent with the hypothesis that human cells expressing full-length human TAP1 and TAP2 contain complexes associated with zero, one, or two MHC I molecules, whereas the truncated TAP mutants only associate with zero or one MHC I molecule.

In a second approach, to confirm that two MHC I molecules may associate with a single human PLC in a subset of complexes, a co-immunoprecipitation study was performed. We expressed CFP-tagged HLA-A2 in HeLaM cells (Fig. 5*A*, *left* and *bottom right panels*), which endogenously express three other MHC I alleles (HLA-A6802, -B1503, and -C1203) and are highly IFN-γ-inducible, allowing augmentation of tapasin and MHC I levels for more effective detection. The 30-kDa CFP tag permits both discrimination of tagged and endogenous MHC I by SDS-PAGE (Fig. 5*A*, *top right panel*) and immunoprecipitation of HLA-A2-containing PLCs using an anti-GFP antibody. After verifying that digitonin lysates of IFN-γ-stimulated HeLaM.A2-CFP cells also exhibit a discrepancy in PaSta1 and PaSta2 binding and that HLA-A2-CFP successfully integrates into the PLC (Fig. 5*B*), PLCs were purified by immunoaffinity chromatography and competitive peptide elution. Anti-GFP immunoprecipitation of the resultant purified material co-precipitated endogenous MHC I (Fig. 5*C*), indicating that both endogenous and untagged MHC I and HLA-A2-CFP may be present within a single PLC.

Digitonin was used to solubilize the PLC because it preserves the relatively weak interactions between PLC components (56). To verify that the co-precipitation of endogenous and CFP-tagged MHC I was not due to PLC aggregation in this mild detergent, the affinity-purified complexes were analyzed by size-exclusion chromatography. Quantitative immunoblotting of the resultant fractions revealed a peak for TAP1 at ~49 ml of the column elution volume, with an estimated Stokes radius of 7.8 nm, between those of thyroglobulin (8.5 nm, 660 kDa) and apoferritin (6.1 nm, 440 kDa) (Fig. 5*D*). Similar results were also obtained using 45.1 and Daudi.β_2m cells (data not shown). The calculated molecular mass of a PLC carrying one or two MHC I molecules is ~468–498 or 584–644 kDa, respectively, depending on whether MHC I is tagged with CFP. Although these values are also consistent with the calibration, the actual molecular weight of the PLC may be higher due to detergent binding. The complexes appeared monodisperse, and there is no evidence that any material was excluded from the column, suggesting that the observed co-precipitation of two MHC I molecules did not stem from PLC aggregation. The results are also consistent with our SiMPull data indicating that PLCs contain two tapasin molecules per TAP heterodimer (Fig. 1), each of which can bind one MHC I molecule.

MHC I Saturation of the PLC Varies with Allele—His-tagged HLA-A2 was expressed in C1R cells (Fig. 6*A*, *left* and *top right panels*), which endogenously exhibit only low levels of HLA-C4 (57) (Fig. 6*A*, *bottom right panel*). HLA-C alleles have been shown to be highly peptide-selective, slowing their release from the PLC (58). As noted for 45.1 cells (Fig. 2*B*) and C1R cells (Fig. 6*B*), when depleting immunoprecipitation was performed on C1R.A2-His digitonin lysate, ~40% of all precipitated MHC I was recognized by PaSta1 but not by PaSta2 (Fig. 6*C*, *right panel*). However, when the individual MHC I alleles were examined by immunoblotting with either HC10, reactive with HLA-B and -C, or an anti-His antibody, we found that ~60% of PLC-associated HLA-C4 was precipitated by PaSta1 alone, while only ~30% of HLA-A2-His was associated with the same PLC subpopulation (Fig. 6*C*, *left panel*). Similarly, ~60% of endogenous MHC I molecules, including HLA-C, and ~20% of CFP-tagged HLA-A2 were precipitated by PaSta1 alone in HeLaM.A2-CFP cells (Fig. 5*B*). These findings suggest that MHC I-saturated PLCs, exhibiting a tapasin/MHC I ratio of 2:2, may reflect protracted retention of peptide-selective MHC I alleles.

MHC I Occupancy of the PLC Increases with Decreased Peptide Supply—To determine whether the average number of MHC I molecules associated with the PLC is stable or dynamic, we performed intracellular flow cytometry on 45.1 cells treated with the proteasome inhibitor lactacystin or expressing the human cytomegalovirus protein US6 (Fig. 7*A*) or the herpes simplex virus protein ICP47, which abrogate ATP and peptide binding to TAP, respectively, blocking peptide transport. This flow cytometry method is sensitive to moderate changes in PLC composition and facilitates direct comparison of cell types. In all cases, the PaSta2/PaSta1 binding ratio decreased when the peptide supply to the ER was reduced (Fig. 7*B*), consistent with increased MHC I association with tapasin, which results in diminished PaSta2 reactivity (Fig. 2*C*). Increased MHC I occupancy of the PLC, indicated by a reduced PaSta2/PaSta1 binding ratio, was also noted in T2 cells expressing TAP1 and/or TAP2 Walker A-motif mutants (1K>A and 2K>A; Fig. 7*C*), which are unable to hydrolyze ATP and are thus transport-incompetent (35). Taken together, these results suggest that decreasing the peptide supply may increase the number of MHC I molecules associated with the PLC, indicating a dynamic stoichiometry that adapts to the peptide supply to the ER.

Lactacystin-treated Daudi and Daudi.β_2m cells were also examined by intracellular flow cytometry to verify that reduced PaSta2 reactivity with tapasin in response to a decreased peptide pool is MHC I-dependent. Whereas the PaSta2/PaSta1 binding ratio in Daudi cells was unaffected (Fig. 7*D*, *left panel*), lactacystin decreased the ratio in Daudi.β_2m cells (Fig. 7*D*, *right panel*), confirming the MHC I dependence of the observed effect.

DISCUSSION

The incorporation of MHC I molecules into the PLC is essential for their acquisition of high affinity peptides (59), which is in turn necessary to mount an effective immune response. Tapasin is critical for optimal MHC I antigen presentation, bridging TAP and MHC I (10), stabilizing and retaining empty MHC I molecules (11, 12), and optimizing MHC I peptide binding (9, 13–17). Yet although the functions of tapasin are increasingly well characterized, its stoichiometry in the PLC has remained

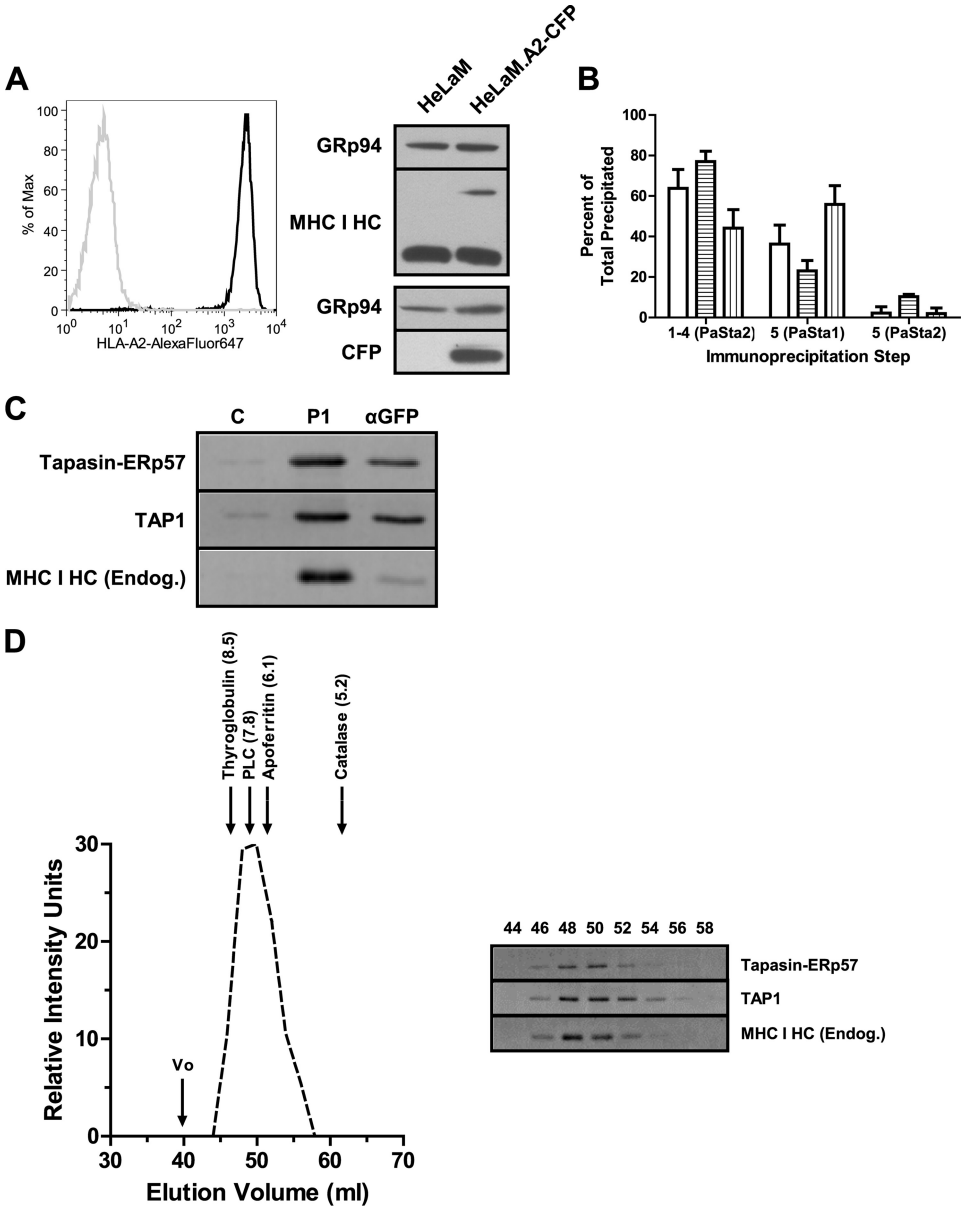

FIGURE 5. **Co-immunoprecipitation and size-exclusion chromatography indicate that two MHC I molecules can associate with a single human PLC.** *A*, HeLaM (*gray line*) and HeLaM.A2-CFP (*black line*) cells were labeled with BB7.2 (anti-HLA-A2) and AlexaFluor647-coupled goat anti-mouse IgG and analyzed by flow cytometry (*left panel*). HeLaM and HeLaM.A2-CFP digitonin lysates were also assessed for MHC I (*top right panel*) and CFP (*bottom right panel*) expression by SDS-PAGE and immunoblotting with 3B10.7 (anti-MHC I HC) and JL-8 (anti-GFP), respectively. Anti-GRp94 was used as a loading control. *B*, HeLaM.A2-CFP digitonin lysate sequentially immunoprecipitated with PaSta2, followed by a fifth immunoprecipitation with PaSta1 or PaSta2. After SDS-PAGE and immunoblotting with R.Gp48C (anti-tapasin), JL-8 (anti-GFP), and 3B10.7 (anti-MHC I HC), the bands were quantitated. These results are expressed as the means plus the S.D. of two independent experiments. *White bars*, tapasin-ERp57. *Horizontally striped bars*, HLA-A2-CFP. *Vertically striped bars*, endogenous MHC I. *C*, HeLaM.A2-CFP digitonin lysate was applied to a 148.3 (anti-TAP1) immunoaffinity column, followed by competitive peptide elution. The resultant affinity-purified PLCs were immunoprecipitated with the indicated antibodies, including the mouse anti-GFP antibody 3E6; separated by SDS-PAGE; and immunoblotted with R.SinA (anti-tapasin), R.RING4C (anti-TAP1), and 3B10.7 (anti-MHC I HC). MaP.IP30 (anti-GILT) served as a negative control for the immunoprecipitation. These results are representative of two independent experiments. *D*, PLCs affinity-purified from HeLaM.A2-CFP digitonin lysate were fractionated by size-exclusion chromatography, and the resultant fractions were immunoblotted with R.SinA (anti-tapasin), R.RING4C (anti-TAP1), and 3B10.7 (anti-MHC I HC) (*right panel*). The Stokes radius of the PLC was then calculated based on the peak fraction for TAP1 and column calibration with proteins of known Stokes radii. Quantitation of the bands (*dashed line*) and calibration proteins (*arrows*) is indicated (*left panel*). The void volume v_0 is also designated by an *arrow*. The Stokes radius values, expressed in nanometers, are cited in *parentheses*. These results are representative of two independent experiments. *HC*, heavy chain. *C*, control antibody. *P1*, PaSta1. *Endog.*, endogenous.

unresolved. Here, using human cell lines and both biophysical and biochemical approaches, we report a TAP/tapasin ratio of 1:2 and PLC subpopulations with tapasin/MHC I ratios of 2:1 and 2:2. Although we do not present direct evidence for a PLC subpopulation lacking MHC I in normal human B cells, our experiments using Daudi cells confirm that such complexes are stable (Fig. 3, *A* and *B*). We also demonstrate that MHC I occupancy of tapasin is allele-dependent and dynamic, changing with peptide supply. These findings improve our understanding of the quality control of MHC I peptide loading and may facilitate structural and functional modeling of the PLC.

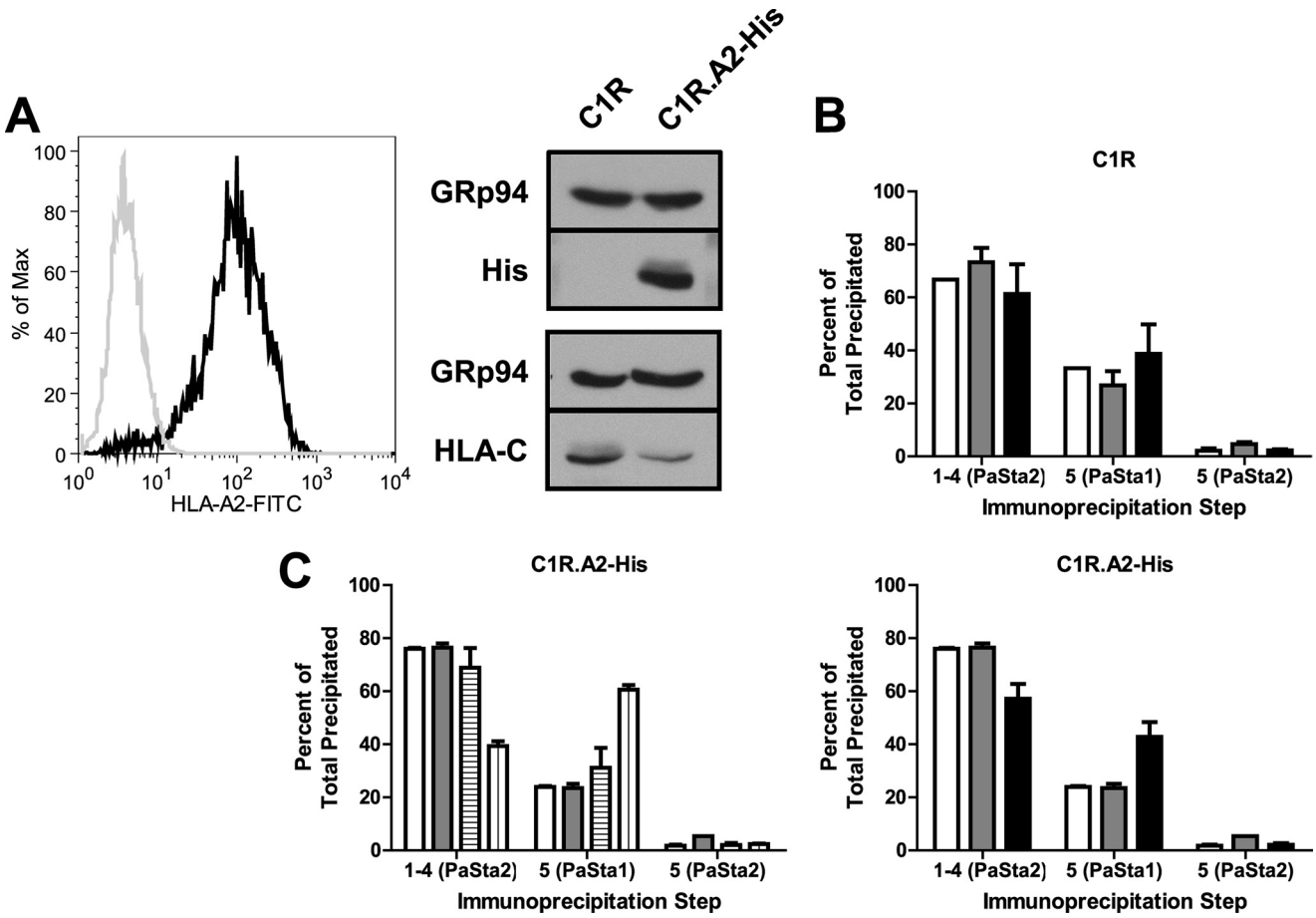

FIGURE 6. **MHC I saturation of the PLC varies with allele.** *A*, C1R.A2-His cells (*black line*) were labeled with BB7.2 (anti-HLA-A2) and FITC-conjugated goat anti-mouse IgG and analyzed for MHC I surface expression in comparison with C1R cells (*gray line*) by flow cytometry (*left panel*). C1R and C1R.A2-His digitonin lysates were also assessed for His and endogenous HLA-C4 expression by SDS-PAGE and immunoblotting with mouse anti-His (*top right panel*) and HC10 (anti-HLA-C HC) (*bottom right panel*), respectively. Anti-GRp94 was used as a loading control. C1R (*B*) and C1R.A2-His (*C*) digitonin lysates were sequentially immunoprecipitated with PaSta2, followed by a fifth immunoprecipitation with PaSta1 or PaSta2. After SDS-PAGE and immunoblotting with R.Gp48C (anti-tapasin), R.RING4C (anti-TAP1), and 3B10.7 (anti-MHC I HC) (for C1R) or rabbit anti-His and HC10 (anti-HLA-C HC) (for C1R.A2-His), the bands were quantitated. Both HLA-A2-His and HLA-C4 (*left panel*) and total MHC I (*right panel*) were plotted for C1R.A2-His. These results are expressed as the means plus the S.D. of two independent experiments. *White bars*, tapasin-ERp57. *Gray bars*, TAP1. *Black bars*, total MHC I. *Horizontally striped bars*, HLA-A2-His. *Vertically striped bars*, endogenous HLA-C4.

Past studies have variously defined the TAP/tapasin/MHC I ratio as 1:1:1 based on velocity sedimentation analysis (23) and 1:4:4 based on quantitation of the amino acid content of affinity-purified complexes (24). These findings were published prior to the discovery of ERp57 association with the PLC (54), potentially skewing stoichiometric calculations. The 1:1 and 1:4 TAP/tapasin ratios were further challenged by reports suggesting two tapasin-binding sites on TAP (5, 6, 25, 26). Consistent with this finding, Rufer *et al.* (21) proposed a mixed TAP/tapasin/MHC I ratio of 1:2:0 and 1:2:1 following blue native-PAGE and antibody-shift analysis, postulating that the two tapasin molecules alternately bind MHC I. However, this study did not take into account possible detergent effects on molecular mass and the limited resolution of its techniques and relied primarily on chimeric human cells expressing rat TAP.

Common approaches to characterizing protein complex stoichiometry, including cryoelectron microscopy and tandem mass spectrometry, are difficult to apply to the PLC due to its heterogeneous composition. SiMPull provides a new means of determining the composition of asymmetric complexes by fluorescently tagging a protein of interest and determining the number present in a single complex by photobleaching (37, 38). Using this method, we confirmed a TAP/tapasin ratio of 1:2 in the .220.B4402.tapasin-YFP human cell line (Fig. 1), consistent with past reports (5, 6, 21, 25, 26). The uniformity of this stoichiometry is supported by intracellular flow cytometry data showing that the anti-TAP1:PaSta1 binding ratio is approximately equal in Daudi and Daudi.β_2m cells and in 45.1 cells and their derivatives (data not shown). Despite the efficacy of SiMPull in identifying the TAP/tapasin ratio, it could not be applied to the more controversial tapasin/MHC I ratio due to a lack of truly MHC I-negative cells in which to express YFP-tagged MHC I. Even in the .221 cell line, which lacks the classical HLA-A, -B, and -C alleles, the nonclassical HLA-E allele still associates with the PLC (60).

To determine the tapasin/MHC I ratio, we utilized the antibody pair PaSta1 and PaSta2 to distinguish between different PLC subpopulations (Figs. 2 and 3), as well as cells expressing N-terminally truncated human TAP or CFP-tagged HLA-A2 to examine MHC I association with tapasin (Figs. 4 and 5). It was previously shown that by truncating the N terminus of either rat TAP1 or TAP2 in T2 cells, tapasin association with the PLC

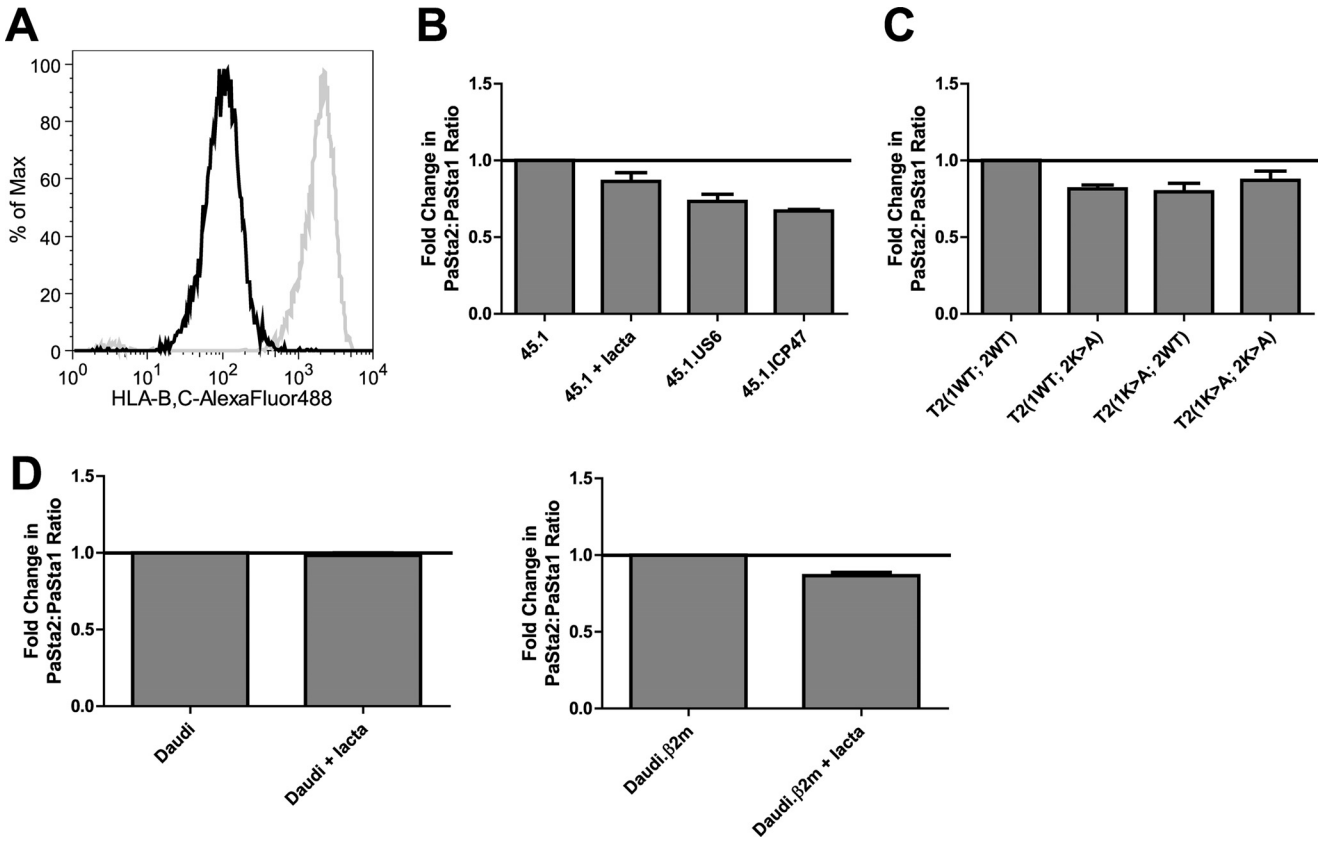

FIGURE 7. **MHC I occupancy of the PLC increases with decreased peptide supply.** *A*, 45.1 (*gray line*) and 45.1.US6 (*black line*) cells were labeled with 4E (anti-HLA-B and -C) and AlexaFluor488-coupled goat anti-mouse IgG and analyzed for MHC I surface expression by flow cytometry. *B*, 45.1, lactacystin-treated 45.1 (20 μM for 2.5 h), 45.1.US6, and 45.1.ICP47 cells were fixed in formaldehyde, permeabilized in saponin, and labeled with PaSta1 or PaSta2 and AlexaFluor488-coupled goat anti-mouse IgG prior to intracellular flow cytometry. A negative control, labeled only with secondary antibody, was also included. The ratio of PaSta2/PaSta1 binding following background subtraction was then calculated. These results are expressed as the means plus the S.D. of three independent experiments. T2(1WT; 2WT), T2(1WT; 2K>A), T2(1K>A; 2WT), and T2(1K>A; 2K>A) (*C*) and Daudi (*left panel*) and Daudi.β_2m (*right panel*) (*D*) cells were similarly analyzed by intracellular flow cytometry. These results are expressed as the means plus the S.D. of two (*C*) or three independent (*D*) experiments. *Lacta*, lactacystin.

was halved, although MHC I association remained the same as in T2 cells expressing full-length rat TAP1 and TAP2 (6). This study suggested a tapasin/MHC I ratio of 2:1, which was subsequently confirmed by Rufer *et al.* (21) but which diverges from our findings using T2 cells expressing truncated human TAP (Fig. 4). The difference in the tapasin/MHC I ratio between human TAP- and rat TAP-expressing T2 cells is supported by increased PaSta2 reactivity with the PLC in the latter (supplemental Fig. S1*A versus* Fig. 4*B* and supplemental Fig. S1*B*), while the TAP/tapasin ratio remains the same (supplemental Fig. S1*C*). Although rat and human TAP share 80% sequence homology, with rat-human chimeric transporters capable of peptide translocation, they do exhibit differences, including disparate sensitivity to the human cytomegalovirus TAP inhibitor US6 (61). Our intracellular flow cytometry studies further demonstrate that multiple TAP functions, including ATP binding and hydrolysis and peptide binding, are required for MHC I dissociation from the human PLC (Fig. 7), while only ATP binding is necessary to trigger MHC I release in rat TAP-expressing T2 cells (62). This disparity in what is required for MHC I dissociation from the PLC, as well as in the tapasin/MHC I ratio, may originate from species-specific differences in the interactions of transporters with any or only human PLC components.

Having established the tapasin/MHC I ratio, we also determined that reducing the peptide supply to the ER by inhibiting the proteasome or blocking TAP-mediated peptide transport increases MHC I occupancy of the PLC (Fig. 7). This finding is in agreement with past reports suggesting that MHC I association with tapasin is prolonged and/or that MHC I maturation is delayed when the peptide pool is diminished by *N*-acetyl-L-leucyl-L-leucyl-L-norleucinal, which inhibits the proteasome (25, 63), the TAP inhibitor US6 (1), Walker A-motif mutation of TAP (2), or the absence of TAP (3). The duration of MHC I binding to the PLC has also been shown to vary with HLA allele (13), including protracted HLA-C binding (58), although this study is the first to report that prolonged MHC I association affects PLC stoichiometry (Figs. 6 and 7).

The relatively low level of PLCs containing two MHC I molecules under normal conditions, ranging from 10 to 40% of the total in various human cell types, is surprising, as MHC I saturation of tapasin seems to be the most efficient means of maximizing high affinity peptide binding (24). However, this low basal level of MHC I saturation may allow PLCs to dynamically adapt to changes in peptide supply, for example during viral infection, increasing the likelihood of effective MHC I antigen binding and presentation. Nevertheless, it is unclear what pre-

vents MHC I from saturating all PLC-associated tapasin under normal conditions, whether in a human or rat-human chimeric cell line. One possibility is that partial saturation reflects a dynamic equilibrium, with more rapid dissociation of MHC I from the complex than association. Alternatively, MHC I binding may be inhibited by a conformational change in tapasin, perhaps mediated by TAP; this could account for the observed rat-human differences in PLC stoichiometry. A third possibility is that an unidentified PLC component occasionally obstructs MHC I binding. Previous studies have reported B-cell receptor-associated protein 31 (64) and protein disulfide isomerase (65) involvement in the PLC, but we and others have not been able to co-precipitate these proteins with other PLC components (19, 21, 66) (data not shown). Although calnexin association with the PLC has also been demonstrated (21, 24, 41), calnexin knockdown does not increase MHC I association with the PLC, as would be expected if the protein typically blocked MHC I binding (data not shown). The mechanism responsible for differential MHC I binding to PLCs containing rat or human TAP thus requires further investigation.

Acknowledgments—We thank Dr. Jeffrey Grotzke, Dr. Crina Paduraru, Dr. Pamela Wearsch, and Wei Zhang for helpful discussions and Susan Mitchell, James Cresswell, and Zhao Zhao for technical assistance. We are also grateful to Dr. Michael Knittler, Dr. David Stepensky, Dr. Nathalie Vigneron, and Dr. Paul Lehner for valuable reagents and to Nancy Dometios for preparation of the manuscript.

REFERENCES

1. Lehner, P. J., Karttunen, J. T., Wilkinson, G. W., and Cresswell, P. (1997) The human cytomegalovirus US6 glycoprotein inhibits transporter associated with antigen processing-dependent peptide translocation. *Proc. Natl. Acad. Sci. U.S.A.* **94,** 6904–6909
2. Knittler, M. R., Alberts, P., Deverson, E. V., and Howard, J. C. (1999) Nucleotide binding by TAP mediates association with peptide and release of assembled MHC class I molecules. *Curr. Biol.* **9,** 999–1008
3. Bangia, N., and Cresswell, P. (2005) Stoichiometric tapasin interactions in the catalysis of major histocompatibility complex class I molecule assembly. *Immunology* **114,** 346–353
4. Hughes, E. A., Hammond, C., and Cresswell, P. (1997) Misfolded major histocompatibility complex class I heavy chains are translocated into the cytoplasm and degraded by the proteasome. *Proc. Natl. Acad. Sci. U.S.A.* **94,** 1896–1901
5. Koch, J., Guntrum, R., Heintke, S., Kyritsis, C., and Tampé, R. (2004) Functional dissection of the transmembrane domains of the transporter associated with antigen processing (TAP). *J. Biol. Chem.* **279,** 10142–10147
6. Leonhardt, R. M., Keusekotten, K., Bekpen, C., and Knittler, M. R. (2005) Critical role for the tapasin-docking site of TAP2 in the functional integrity of the MHC class I-peptide-loading complex. *J. Immunol.* **175,** 5104–5114
7. Bangia, N., Lehner, P. J., Hughes, E. A., Surman, M., and Cresswell, P. (1999) The N-terminal region of tapasin is required to stabilize the MHC class I loading complex. *Eur. J. Immunol.* **29,** 1858–1870
8. Garbi, N., Tiwari, N., Momburg, F., and Hämmerling, G. J. (2003) A major role for tapasin as a stabilizer of the TAP peptide transporter and consequences for MHC class I expression. *Eur. J. Immunol.* **33,** 264–273
9. Lehner, P. J., Surman, M. J., and Cresswell, P. (1998) Soluble tapasin restores MHC class I expression and function in the tapasin-negative cell line. 220. *Immunity* **8,** 221–231
10. Sadasivan, B., Lehner, P. J., Ortmann, B., Spies, T., and Cresswell, P. (1996) Roles for calreticulin and a novel glycoprotein, tapasin, in the interaction of MHC class I molecules with TAP. *Immunity* **5,** 103–114
11. Grandea, A. G., 3rd, Lehner, P. J., Cresswell, P., and Spies, T. (1997) Regulation of MHC class I heterodimer stability and interaction with TAP by tapasin. *Immunogenetics* **46,** 477–483
12. Barnden, M. J., Purcell, A. W., Gorman, J. J., and McCluskey, J. (2000) Tapasin-mediated retention and optimization of peptide ligands during the assembly of class I molecules. *J. Immunol.* **165,** 322–330
13. Williams, A. P., Peh, C. A., Purcell, A. W., McCluskey, J., and Elliott, T. (2002) Optimization of the MHC class I peptide cargo is dependent on tapasin. *Immunity* **16,** 509–520
14. Howarth, M., Williams, A., Tolstrup, A. B., and Elliott, T. (2004) Tapasin enhances MHC class I peptide presentation according to peptide half-life. *Proc. Natl. Acad. Sci. U.S.A.* **101,** 11737–11742
15. Wearsch, P. A., and Cresswell, P. (2007) Selective loading of high affinity peptides onto major histocompatibility complex class I molecules by the tapasin-ERp57 heterodimer. *Nat. Immunol.* **8,** 873–881
16. Chen, M., and Bouvier, M. (2007) Analysis of interactions in a tapasin-class I complex provides a mechanism for peptide selection. *EMBO J.* **26,** 1681–1690
17. Praveen, P. V., Yaneva, R., Kalbacher, H., and Springer, S. (2010) Tapasin edits peptides on MHC class I molecules by accelerating peptide exchange. *Eur. J. Immunol.* **40,** 214–224
18. Wearsch, P. A., Peaper, D. R., and Cresswell, P. (2011) Essential glycan-dependent interactions optimize MHC class I peptide loading. *Proc. Natl. Acad. Sci. U.S.A.* **108,** 4950–4955
19. Peaper, D. R., Wearsch, P. A., and Cresswell, P. (2005) Tapasin and ERp57 form a stable disulfide-linked dimer within the MHC class I peptide-loading complex. *EMBO J.* **24,** 3613–3623
20. Peaper, D. R., and Cresswell, P. (2008) The redox activity of ERp57 is not essential for its functions in MHC class I peptide loading. *Proc. Natl. Acad. Sci. U.S.A.* **105,** 10477–10482
21. Rufer, E., Leonhardt, R. M., and Knittler, M. R. (2007) Molecular architecture of the TAP-associated MHC class I peptide-loading complex. *J. Immunol.* **179,** 5717–5727
22. Meyer, T. H., van Endert, P. M., Uebel, S., Ehring, B., and Tampé, R. (1994) Functional expression and purification of the ABC transporter complex associated with antigen processing (TAP) in insect cells. *FEBS Lett.* **351,** 443–447
23. Li, S., Sjögren, H. O., Hellman, U., Pettersson, R. F., and Wang, P. (1997) Cloning and functional characterization of a subunit of the transporter associated with antigen processing. *Proc. Natl. Acad. Sci. U.S.A.* **94,** 8708–8713
24. Ortmann, B., Copeman, J., Lehner, P. J., Sadasivan, B., Herberg, J. A., Grandea, A. G., Riddell, S. R., Tampé, R., Spies, T., Trowsdale, J., and Cresswell, P. (1997) A critical role for tapasin in the assembly and function of multimeric MHC class I-TAP complexes. *Science* **277,** 1306–1309
25. Antoniou, A. N., Ford, S., Pilley, E. S., Blake, N., and Powis, S. J. (2002) Interactions formed by individually expressed TAP1 and TAP2 polypeptide subunits. *Immunology* **106,** 182–189
26. Hulpke, S., Tomioka, M., Kremmer, E., Ueda, K., Abele, R., and Tampe, R. (2012) Direct evidence that the N-terminal extensions of the TAP complex act as autonomous interaction scaffolds for the assembly of the MHC I peptide-loading complex. *Cell. Mol. Life Sci.*, in press
27. Peh, C. A., Burrows, S. R., Barnden, M., Khanna, R., Cresswell, P., Moss, D. J., and McCluskey, J. (1998) HLA-B27-restricted antigen presentation in the absence of tapasin reveals polymorphism in mechanisms of HLA class I peptide loading. *Immunity* **8,** 531–542
28. DeMars, R., Chang, C. C., Shaw, S., Reitnauer, P. J., and Sondel, P. M. (1984) Homozygous deletions that simultaneously eliminate expressions of class I and class II antigens of EBV-transformed B-lymphoblastoid cells. I. Reduced proliferative responses of autologous and allogeneic T cells to mutant cells that have decreased expression of class II antigens. *Hum. Immunol.* **11,** 77–97
29. Klein, E., Klein, G., Nadkarni, J. S., Nadkarni, J. J., Wigzell, H., and Clifford, P. (1968) Surface IgM-κ specificity on a Burkitt lymphoma cell *in vivo* and in derived culture lines. *Cancer Res.* **28,** 1300–1310
30. Seong, R. H., Clayberger, C. A., Krensky, A. M., and Parnes, J. R. (1988) Rescue of Daudi cell HLA expression by transfection of the mouse β_2-

microglobulin gene. *J. Exp. Med.* **167,** 288–299
31. Salter, R. D., Howell, D. N., and Cresswell, P. (1985) Genes regulating HLA class I antigen expression in T-B lymphoblast hybrids. *Immunogenetics* **21,** 235–246
32. Edwards, P. A., Smith, C. M., Neville, A. M., and O'Hare, M. J. (1982) A human-hybridoma system based on a fast-growing mutant of the ARH-77 plasma cell leukemia-derived line. *Eur. J. Immunol.* **12,** 641–648
33. DuBridge, R. B., Tang, P., Hsia, H. C., Leong, P. M., Miller, J. H., and Calos, M. P. (1987) Analysis of mutation in human cells by using an Epstein-Barr virus shuttle system. *Mol. Cell. Biol.* **7,** 379–387
34. Kusari, J., and Sen, G. C. (1986) Regulation of synthesis and turnover of an interferon-inducible mRNA. *Mol. Cell. Biol.* **6,** 2062–2067
35. Karttunen, J. T., Lehner, P. J., Gupta, S. S., Hewitt, E. W., and Cresswell, P. (2001) Distinct functions and cooperative interaction of the subunits of the transporter associated with antigen processing (TAP). *Proc. Natl. Acad. Sci. U.S.A.* **98,** 7431–7436
36. Momburg, F., Ortiz-Navarrete, V., Neefjes, J., Goulmy, E., van de Wal, Y., Spits, H., Powis, S. J., Butcher, G. W., Howard, J. C., Walden, P., *et al.* (1992) Proteasome subunits encoded by the major histocompatibility complex are not essential for antigen presentation. *Nature* **360,** 174–177
37. Jain, A., Liu, R., Ramani, B., Arauz, E., Ishitsuka, Y., Ragunathan, K., Park, J., Chen, J., Xiang, Y. K., and Ha, T. (2011) Probing cellular protein complexes using single-molecule pull-down. *Nature* **473,** 484–488
38. Jain, A., Liu, R., Xiang, Y. K., and Ha, T. (2012) Single-molecule pull-down for studying protein interactions. *Nat. Protoc.* **7,** 445–452
39. Dick, T. P., Bangia, N., Peaper, D. R., and Cresswell, P. (2002) Disulfide bond isomerization and the assembly of MHC class I-peptide complexes. *Immunity* **16,** 87–98
40. Dong, G., Wearsch, P. A., Peaper, D. R., Cresswell, P., and Reinisch, K. M. (2009) Insights into MHC class I peptide loading from the structure of the tapasin-ERp57 thiol oxidoreductase heterodimer. *Immunity* **30,** 21–32
41. Diedrich, G., Bangia, N., Pan, M., and Cresswell, P. (2001) A role for calnexin in the assembly of the MHC class I loading complex in the endoplasmic reticulum. *J. Immunol.* **166,** 1703–1709
42. Lutz, P. M., and Cresswell, P. (1987) An epitope common to HLA class I and class II antigens, Ig light chains, and β_2-microglobulin. *Immunogenetics* **25,** 228–233
43. Trapani, J. A., Mizuno, S., Kang, S. H., Yang, S. Y., and Dupont, B. (1989) Molecular mapping of a new public HLA class I epitope shared by all HLA-B and HLA-C antigens and defined by a monoclonal antibody. *Immunogenetics* **29,** 25–32
44. Parham, P., and Brodsky, F. M. (1981) Partial purification and some properties of BB7.2. A cytotoxic monoclonal antibody with specificity for HLA-A2 and a variant of HLA-A28. *Hum. Immunol.* **3,** 277–299
45. Stam, N. J., Spits, H., and Ploegh, H. L. (1986) Monoclonal antibodies raised against denatured HLA-B locus heavy chains permit biochemical characterization of certain HLA-C locus products. *J. Immunol.* **137,** 2299–2306
46. Barnstable, C. J., Jones, E. A., and Crumpton, M. J. (1978) Isolation, structure, and genetics of HLA-A, -B, -C, and -DRw (Ia) antigens. *Br. Med. Bull.* **34,** 241–246
47. Arunachalam, B., Pan, M., and Cresswell, P. (1998) Intracellular formation and cell surface expression of a complex of an intact lysosomal protein and MHC class II molecules. *J. Immunol.* **160,** 5797–5806
48. Powis, S. J., Townsend, A. R., Deverson, E. V., Bastin, J., Butcher, G. W., and Howard, J. C. (1991) Restoration of antigen presentation to the mutant cell line RMA-S by an MHC-linked transporter. *Nature* **354,** 528–531
49. Stepensky, D., Bangia, N., and Cresswell, P. (2007) Aggregate formation by ERp57-deficient MHC class I peptide-loading complexes. *Traffic* **8,** 1530–1542
50. Hewitt, E. W., Gupta, S. S., and Lehner, P. J. (2001) The human cytomegalovirus gene product US6 inhibits ATP binding by TAP. *EMBO J.* **20,** 387–396
51. Peaper, D. R., and Cresswell, P. (2008) Regulation of MHC class I assembly and peptide binding. *Annu. Rev. Cell Dev. Biol.* **24,** 343–368
52. Ulbrich, M. H., and Isacoff, E. Y. (2007) Subunit counting in membrane-bound proteins. *Nat. Methods* **4,** 319–321
53. Plewnia, G., Schulze, K., Hunte, C., Tampé, R., and Koch, J. (2007) Modulation of the antigenic peptide transporter TAP by recombinant antibodies binding to the last five residues of TAP1. *J. Mol. Biol.* **369,** 95–107
54. Hughes, E. A., and Cresswell, P. (1998) The thiol oxidoreductase ERp57 is a component of the MHC class I peptide-loading complex. *Curr. Biol.* **8,** 709–712
55. Keusekotten, K., Leonhardt, R. M., Ehses, S., and Knittler, M. R. (2006) Biogenesis of functional antigenic peptide transporter TAP requires assembly of pre-existing TAP1 with newly synthesized TAP2. *J. Biol. Chem.* **281,** 17545–17551
56. Ortmann, B., Androlewicz, M. J., and Cresswell, P. (1994) MHC class I/β_2-microglobulin complexes associate with TAP transporters before peptide binding. *Nature* **368,** 864–867
57. Zemmour, J., Little, A. M., Schendel, D. J., and Parham, P. (1992) The HLA-A,B "negative" mutant cell line C1R expresses a novel HLA-B35 allele, which also has a point mutation in the translation initiation codon. *J. Immunol.* **148,** 1941–1948
58. Neisig, A., Melief, C. J., and Neefjes, J. (1998) Reduced cell surface expression of HLA-C molecules correlates with restricted peptide binding and stable TAP interaction. *J. Immunol.* **160,** 171–179
59. Tan, P., Kropshofer, H., Mandelboim, O., Bulbuc, N., Hämmerling, G. J., and Momburg, F. (2002) Recruitment of MHC class I molecules by tapasin into the transporter associated with antigen processing-associated complex is essential for optimal peptide loading. *J. Immunol.* **168,** 1950–1960
60. Braud, V. M., Allan, D. S., Wilson, D., and McMichael, A. J. (1998) TAP- and tapasin-dependent HLA-E surface expression correlates with the binding of an MHC class I leader peptide. *Curr. Biol.* **8,** 1–10
61. Halenius, A., Momburg, F., Reinhard, H., Bauer, D., Lobigs, M., and Hengel, H. (2006) Physical and functional interactions of the cytomegalovirus US6 glycoprotein with the transporter associated with antigen processing. *J. Biol. Chem.* **281,** 5383–5390
62. Alberts, P., Daumke, O., Deverson, E. V., Howard, J. C., and Knittler, M. R. (2001) Distinct functional properties of the TAP subunits coordinate the nucleotide-dependent transport cycle. *Curr. Biol.* **11,** 242–251
63. Hughes, E. A., Ortmann, B., Surman, M., and Cresswell, P. (1996) The protease inhibitor, *N*-acetyl-L-leucyl-L-leucyl-leucyl-L-norleucinal, decreases the pool of major histocompatibility complex class I-binding peptides and inhibits peptide trimming in the endoplasmic reticulum. *J. Exp. Med.* **183,** 1569–1578
64. Paquet, M. E., Cohen-Doyle, M., Shore, G. C., and Williams, D. B. (2004) Bap29/31 influences the intracellular traffic of MHC class I molecules. *J. Immunol.* **172,** 7548–7555
65. Park, B., Lee, S., Kim, E., Cho, K., Riddell, S. R., Cho, S., and Ahn, K. (2006) Redox regulation facilitates optimal peptide selection by MHC class I during antigen processing. *Cell* **127,** 369–382
66. Kienast, A., Preuss, M., Winkler, M., and Dick, T. P. (2007) Redox regulation of peptide receptivity of major histocompatibility complex class I molecules by ERp57 and tapasin. *Nat. Immunol.* **8,** 864–872